

2-D Seismic Refraction Tomography Investigation of a Sewage Treatment Site

Ahmed I.I.^{1*}, Osazuwa I.B.² and Lawal K.M.³

1. Department of Geology, Ahmadu Bello University Zaria, Nigeria
 2. Department of Physics, Federal University of Petroleum Efurun, Nigeria
 3. Department of Physics, Ahmadu Bello University Zaria, Nigeria
- * E-mail of the corresponding author: ahmedish002@yahoo.com

Abstract

Geophysical investigation involving seismic refraction tomography (SRT) was conducted at a sewage treatment site located at Ahmadu Bello University Zaria with the objectives of determining the overburden thickness and velocity of the subsurface layers in the area, and delineating any geological structures, such as fracture zone, that may pose a threat to the safe running of the Sewage lagoon system in the area. Five seismic profiles, with three running N-S and two running E-W, were acquired over the earthen-dikes separating the lagoons with the aid of a 24-channel digital Seismograph and a 5 kg sledge hammer striking a rubber plate. Tomography models were generated for each of the profiles with the aid of ray tracing through a wave-front inversion method that is based on finite difference approximation of the eikonal equation. Geological artifacts, as a result of noise observed in the tomography models of some of the profiles, were removed by filtrations that include manual editing of model's physical parameters and iterative model updating through simultaneous iterative reconstruction techniques (SIRT). The result of the investigation shows that the area consists of three subsurface layers; an undifferentiated overburden layer with a P-wave velocity range of 891 m/s to 1421 m/s, a partially weathered zone with P-wave velocity range of 3010 m/s to 5129 m/s and underlying fresh granitic basement with P-wave velocity range of 5704 m/s to 7762 m/s, while the overburden thickness in the area varies from an average of about 18 m in the northern part to about 55 m in the southern part. The investigation also revealed a fracture zone within the underlying granitic basement, which occurs at about 60 m below the earthen-dike located at the centre of the study area.

Keywords: 2-D Seismic, Refraction, Tomography, Sewage Lagoon

1.0 Introduction

Ahmadu Bello University Zaria's sewage treatment system utilizes the Sewage lagoon method to collect, convey, treat and dispose wastewater from its community. It is located within the Samaru main campus of Ahmadu Bello University Zaria at latitude $11^{\circ} 8.252^1\text{N}$ and longitude $07^{\circ} 39.535^1\text{E}$, and consists of a septic tank and six ponds that are about 2 m deep, unlined, separated and protected on all sides by earthen dikes (figure 1).

1.1 Aim and Objectives

This research is aimed at conducting a geophysical investigation of the study area for foundation problems such as fracture zones or permeable zones that may pose a threat to the safe running of the Sewage lagoon system in the area, with the following main objectives:

- i) To determine the velocity of the subsurface layers in the study area.
- ii) To determine the thickness of the overburden sediments and the depth to the fresh crystalline basement in the study area.
- iii) To identify and delineate possible fracture and permeable zones that may serve as pathways for leakage and groundwater contamination.

1.2 Site description

The geological investigation of the study area reveals that the area is underlain by rock of the Older Granite that forms part of the Zaria granitic Batholith (Ike 1998). Although there is no outcrop exposure of the granite in the study area, lateritic soil derived from its weathering is well exposed around the northeastern part of the study area. This lateritic soil measures about 3 m in thickness and varies from a more hardened and less compacted layer at the top to a less hardened and more compacted layer below (figure 2). Dominant structural trends in the granitic Batholith of Zaria are almost in the N-S direction, conforming to the Pan-African Orogeny structural trend (Ike 1998). The study area is also characterized by a topography that is gently sloping from its northern part towards the southern part.

1.3 Field work and Data collection

The field work was carried-out with the aid of ABEM 24 channel Seismograph, two geophone groups of 12 geophones each, a 10 kg sledge hammer and a rubber plate, a compass, and a global positioning system (GPS).

A preliminary site survey was first carried out in the study area, part of which include geological investigation of the study area, mapping out appropriate profile lines and determining the azimuth of these profiles with the aid of a compass

Five seismic refraction profiles namely; L1, L2, L3, L4 and L5 were acquired over the earthen-dikes in the study area, with profiles; L1, L2 and L3 running almost N-S direction and L3 and L4 running almost E-W direction as shown in figure 3. There was also the need to check the sensitivity of the instrument, therefore an additional profile, L6, running N-S was acquired over the lateritic soil exposure adjacent to the study area making a total of six profiles acquired. Two geophone groups of 12 geophones each were spread linearly at 5 m intervals with an offset of 40 m at both ends covering a total length of 200 m in each case. Where the length of the earthen-dikes exceeds 200 m as in profile L1 and L2, which has a length of about 300 m each, an overlap of two spreads at 100 m was employed for continuous coverage. Shots were fired with the aid of a sledge hammer striking a rubber plate at 2.5 m intervals within the offsets and the geophone spread in order to have maximum coverage of the subsurface for the purpose of tomography. Vertical stacking, involving the average of several records from five shots at each shooting point, was employed during the data acquisition to improve the signal to noise ratio.

1.4 Precautions

Maintaining good electrical contact between the geophones, the cable wire and the seismographs, and ensuring that the geophones are firmly placed in the ground, in order to achieve good contact for excellent signal detection, were among the precautions taken during the data acquisition. Other precautions include; avoiding body or any contact with the trigger geophone and checking to ensure that all the geophones are intact and responding prior to shooting. In addition the study area is less built-up, limiting the signal interference as a result of noise.

1.5 Methodology

Seismic refraction tomography, involving ray tracing through a wave-front inversion that uses the finite difference approximation of the eikonal equation was employed in this investigation, while iterative model updating, using simultaneous iterative reconstruction techniques (SIRT), was employed in the smoothing of the tomography models.

1.6 Data Processing

A total of 15,680 refraction data acquired during the survey were processed and interpreted with the aid of ReflexW (version 4.6). The data, which were initially acquired in SEG format, was later converted to Reflex format after importing from the Seismograph's storage disk memory. 1-D band pass frequency filter, using upper and lower cutoff

frequency of 150 Hz and 50 Hz respectively, was applied to remove the effect of ground-roll and improve signal-noise ratio. This was followed by manual gain to improve the amplitude of the weak refracted signal and to scale the amplitude so that they are nearly constant in a selected time window. Figure 4a and 4b shows the data before and after filtering respectively, while figure 5a and 5b shows the data before gain and after gain respectively.

The next step was the picking of first arrival-times for each of the trace, which was done manually in the “pick” window. This was then followed with the assignment of these travel-times to layers, which was done by determining the average of the travel-time values corresponding to the points where refraction occurs in the T-X plots for the forward and the reverse shots. The travel-times lower than the average values determined was assigned to the first layer, while the travel-times higher than the average value determined was assigned to the second layer. An illustration of this is shown in figure 6a and 6b.

The layer assignment was followed by the generation of an initial 2-D tomography model, which was carried-out through wave-front inversion and ray-tracing method. The schematic outline of data processing for the tomography is shown in figure 7.

1.7 Data Interpretation

The profile L6 acquired above the exposed lateritic soil adjacent to the study area was the first to be processed and interpreted, in order to serve as a processing and interpretation guide for subsequent profiles acquired in the study area. The initial 2-D tomography model and the corresponding ray-trace generated for this profile is shown in figure 8a. This was then iterated ten times to obtain a final model shown in figure 8b.

The final model revealed some interesting velocity anomalies towards the northern and southern part of the profile, which can be described geologically as a dyke or outcrop exposure of the underlying granitic basement. Meanwhile, there is no dyke or outcrop exposure at the surface along the profile as verified by the geological investigation carried out in the area. This false anomaly may have been caused by a high P-wave velocity among the physical parameters generated for the first layer of the initial 2-D model. This anomalous P-wave velocity (in italics in Table 1) was noticed to be too high (higher than the P-wave velocity of the second layer) and inconsistent with other P-wave velocities generated for the first layer of the model. This is probably a velocity artifact as a result of noise. This high P-wave value was also noticed to have caused the compression of the rays within the region towards the northern part of the profile, such that they appear to have originated from the same point (figure 8a).

In order to remove this anomalous high P-wave velocity, manual editing of the physical parameters was carried out before iterations. This was done by finding the average of the P-wave values corresponding to the immediate distance before and after the distance where the anomalous high P-wave was noticed, and assigning the resultant average P-wave value to this distance. After manual editing, ray tracing was repeated for the edited model parameters, which is shown in figure 9a. This was then followed by five iterations and, subsequently, ten iterations to obtain a 2-D tomography model and final 2-D velocity model shown respectively in figure 9b and 9c.

Similar effect was noticed in profile L4, where a high P-wave, among the physical parameters of the first layer, was observed in the 2-D initial velocity section to have given rise to dike-like structures in figure 10a. After manual editing and ten iterations, the resultant 2-D velocity model, devoid of noise, shows no dike-like structures (figure 10b).

Profile L1 shows extremely high overburden thickness towards the southern part (figure 11b), which was observed to have been caused by lack of ray reaching the second layer as shown in the initial model in figure 11a. This may be due to offset effect or, probably, the energy of the seismic rays was too low to reach the second layer, which resulted to a velocity extrapolation for that region.

Only profile L5 shows anomalous low velocity region within the underlying granitic basement in the study area. This region, which occurs towards the western part of the profile, is suspected to be a fractured zone having a P-wave velocity range of 3,132 m/s to 3,647 m/s. The overburden layer above this zone also appears to be thicker compare to other region along the profile, probably as a result of an intense weathering of the underlying granitic basement aided by the fracture zone shown in the 2-D velocity section in figure 12b.

All the profiles show an overburden layer with P-wave velocity ranging from 891 m/s to 1,421 m/s, a transition zone corresponding to a region of partial weathering with a P-wave velocity range of 3,010 m/s to 5,129 m/s and unweathered, fresh granitic basement underlying the study area with a P-wave velocity range of 5,704 m/s to 7,762 m/s. The 2-D velocity sections, with their corresponding ray-trace, for profile L2 and L3 are shown in figure 13 and 14 respectively, while Table 2 shows the summary of the overburden layer thickness for all the five profiles.

1.8 Discussion and Summary

All the five profiles acquired in the study area revealed the subsurface layers to be made up of a weathered overburden layer, a zone of partial weathering, and underlying fresh granitic basement.

The occasional high P-wave velocity giving rise to geological artifacts noticed in some of the profiles may have been caused by noise in the data, which was removed by filtering through manual editing of model parameters and iterations of tomography models.

The non-resolution of the heterogeneity of the overburden sediment could be noticed as one of the limitations of the method employed in this investigation as the overburden (in blue color in all the profile) is treated as a uniform entity, which is not geologically true in reality.

The effect of not choosing the right offset distance and appropriate energy input in refraction survey could also be noticed in profile L1, where the overburden thickness appears to be extremely high (or infinite) towards the southern part as a result of lack of ray coverage that resulted to a velocity extrapolation for that region of the profile. The offset distance employed in this investigation was chosen based on the previous work conducted by Ososami (1968) and Shemang (1992) around the study area, where, using electrical resistivity method, they proposed the depth to basement around the study area to vary between 5 m to 33 m and 3 m to 44 m respectively, while the energy source from the 5 kg hammer might be too low to reach the second layer. Although subject to availability of borehole data, this investigation has proven to some extent that the overburden thickness and the depth to the crystalline basement in the study area could be probably up to 60 m or more especially towards its southern part.

Among all the five profiles, only profile L5 revealed the occurrence of fracture zone within the underlying granitic basement in the study area, there is possibility that it may serve as a conduit or pathway through which sewage effluents can flow. This can lead to groundwater contamination within and around the study area, when groundwater drains through this fracture during decline in groundwater level especially in dry season.

1.9 Conclusions and Recommendation

It can be concluded that the study area consists of three subsurface layers; an undifferentiated overburden layer with a P-wave velocity range of 891 m/s to 1,421 m/s, a partially weathered zone with P-wave velocity range of 3,010 m/s to 5,129 m/s and underlying fresh granitic basement with P-wave velocity range of 5,704 m/s to 7,762 m/s.

The thickness of the undifferentiated, overburden layer varies within the study area from an average of 18 m in the northern part to 55 m in the southern part.

Fracture zone occurs within the underlying granitic basement at about 60 m beneath and towards the eastern part of the earthen-dike located at the centre of the study area.

Fracture poses a great threat to the safe running of Sewage lagoon system. It can lead to the failure of the Sewage lagoon system by serving as pathways through which groundwater can be contaminated by sewage effluent; therefore, it is recommended that the lagoons are lined at the base with impermeable materials to prevent the draining of the sewage effluent through the fracture zone occurring at the depth of 60 m beneath and towards the western part of the Sewage lagoon system.

2.0 Acknowledgement

This project was financed by the International Programme on Physical Sciences (IPPS), University of Uppsala,

Uppsala Sweden.

REFERENCES

- Ike, E. C. (1988), *Late-stage Geological Phenomena in the Zaria Basement Granites*, In Precambrian Geology of Nigeria, Geological Survey of Nigeria Spec. Pub. pp. 83-89.
- Ososami, A. I. (1968), *Assessment of the Groundwater in the Kubanni valley, Zaria*. An Unpublished M.Sc. Thesis, Department of Civil Engineering, A. B. U. Zaria.
- Shemang, E.M., Ajayi, C.O. and Osazuwa, I.B. (1992). *The Basement Rocks and Tectonism in the Kubanni River Basin, Zaria Nigeria: Deductions from D.C. Resistivity Data*. Journal of Mining and Geology, Vol. 28; No.1, pp. 119-124.



Figure 1: Location of the study area (Google satellite image, 2009).



Figure 2: Lateritic soil exposed around the study area, measuring about 3 m in thickness

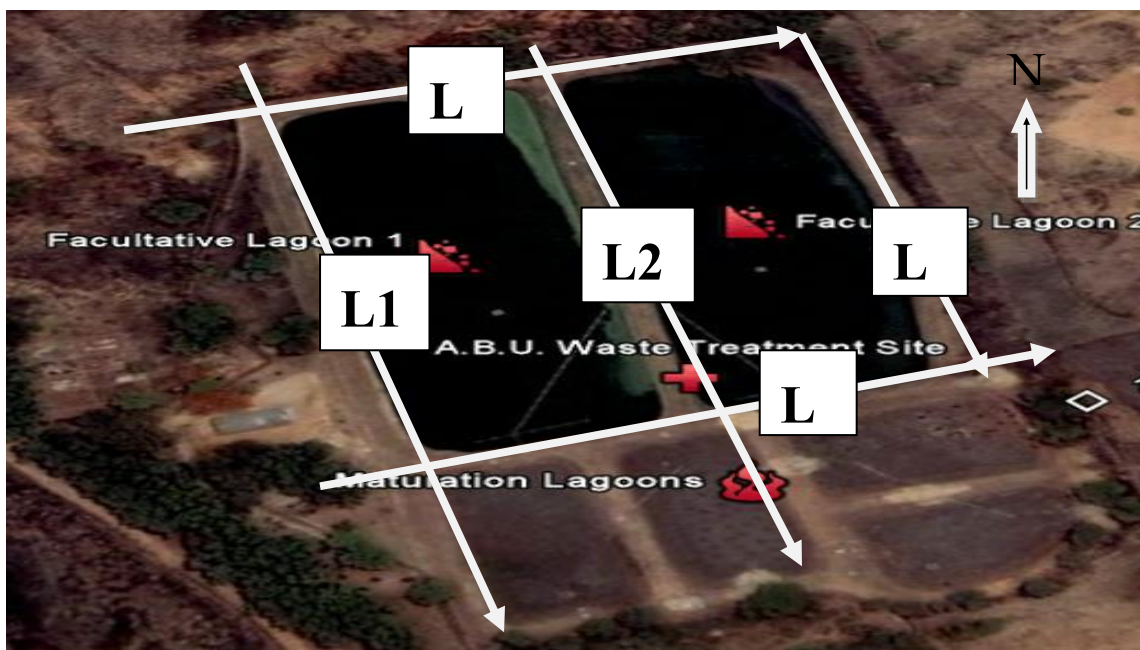


Figure 3: Seismic profiles acquired in the study area, azimuths are indicated by the direction of arrows.

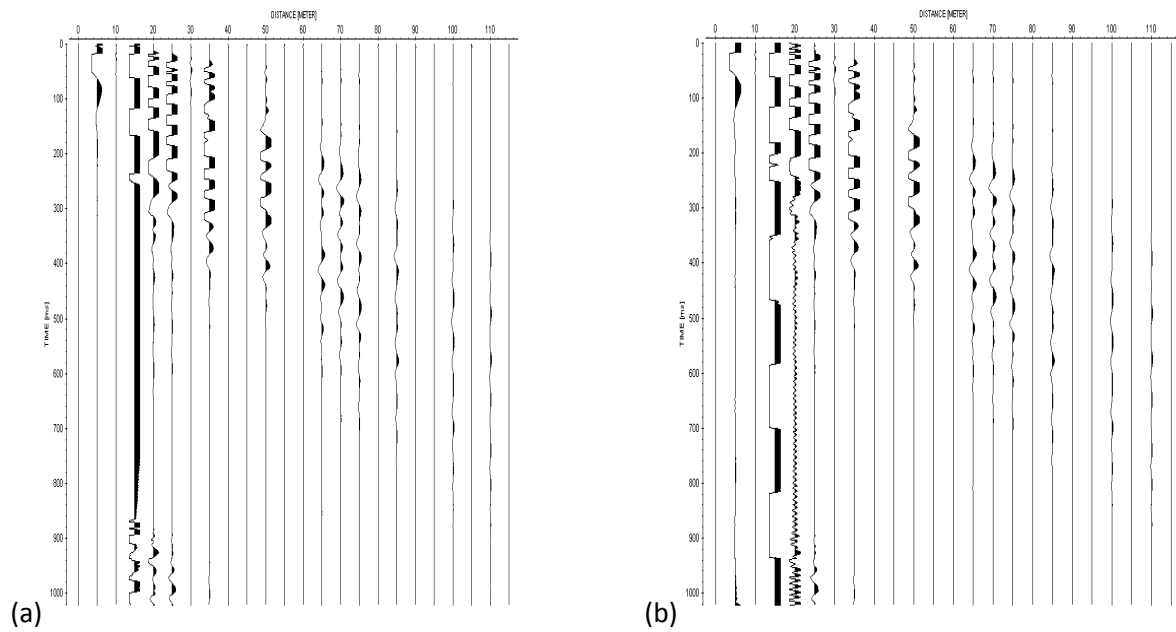


Figure 4: The data (a) before filtering and (b) after filtering.

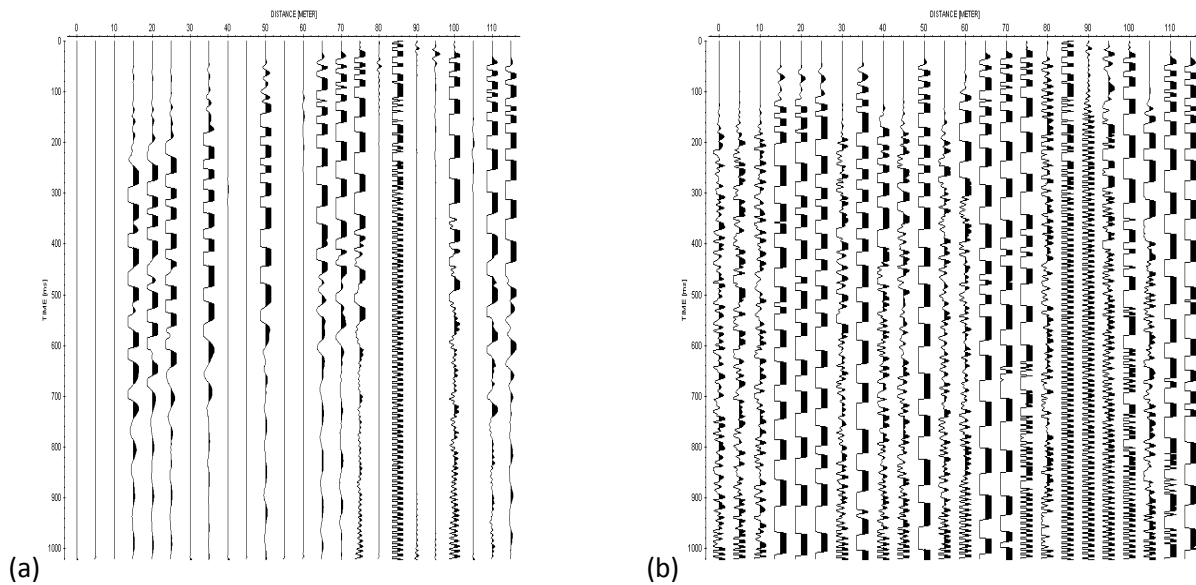


Figure 5: The data (a) before gain and (b) after gain

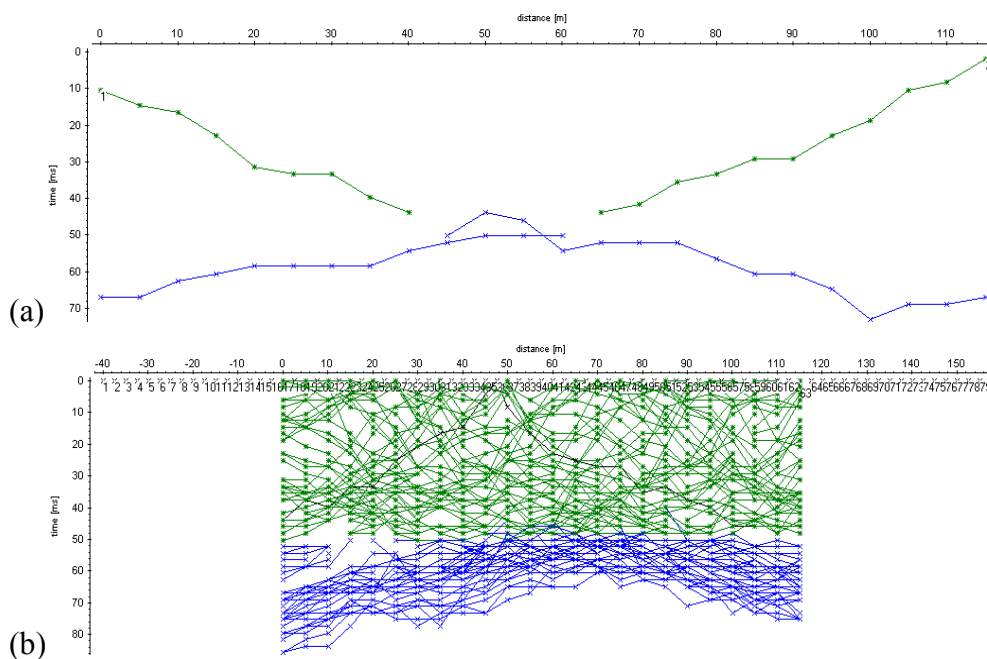
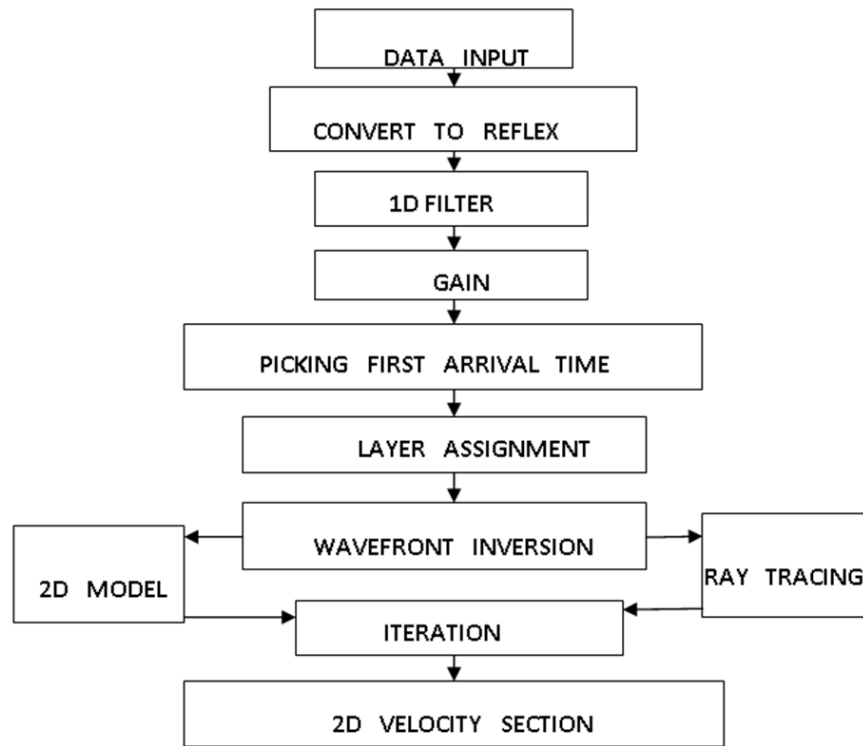


Figure 6: An illustration of layer assignment: (a) finding the average of the travel-times; (b) assigning values to layers; first layer (green) and second layer (blue).



SW

Figure 7: Flowchart for the refraction tomography data processing.

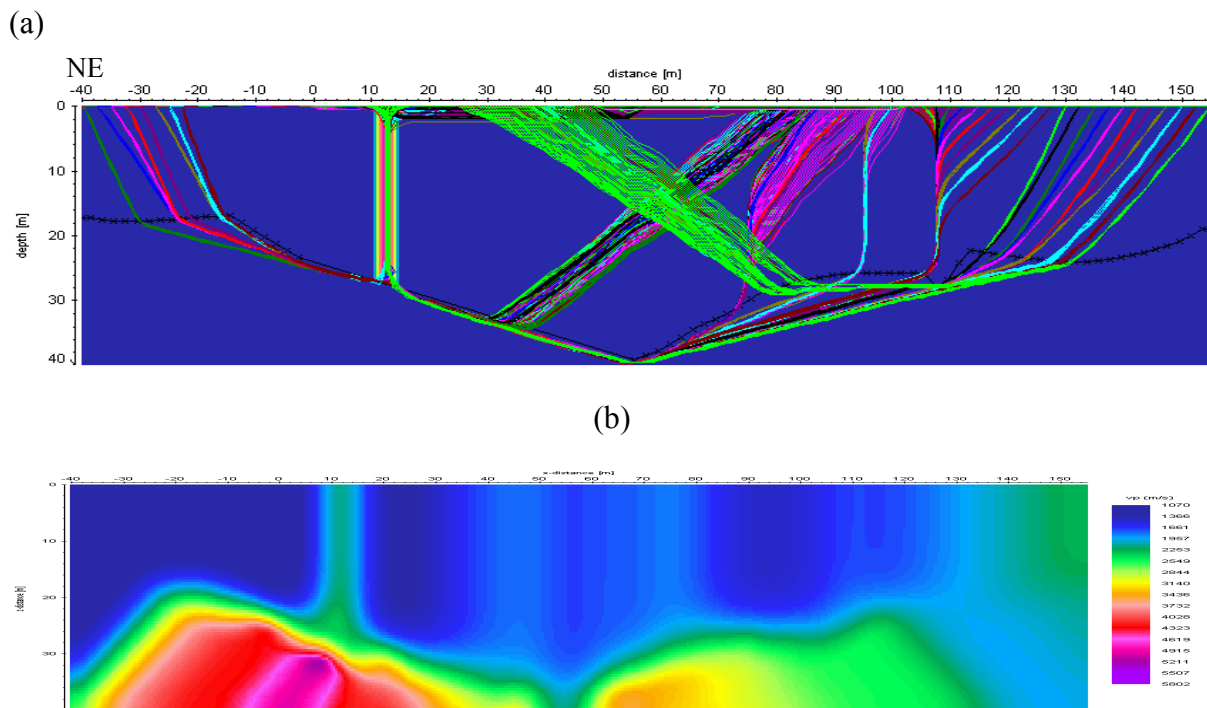
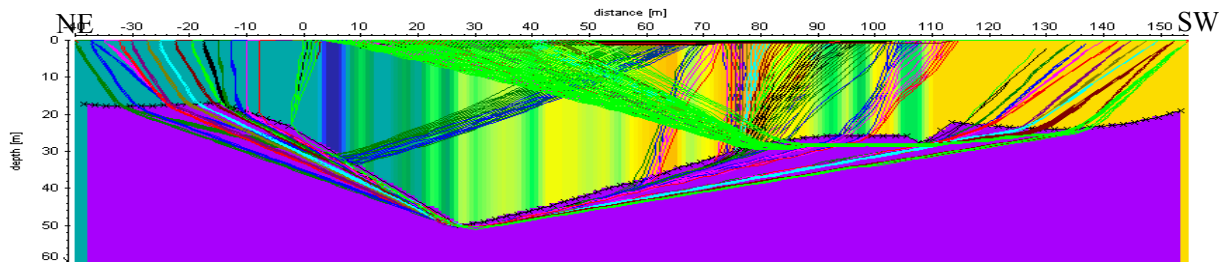
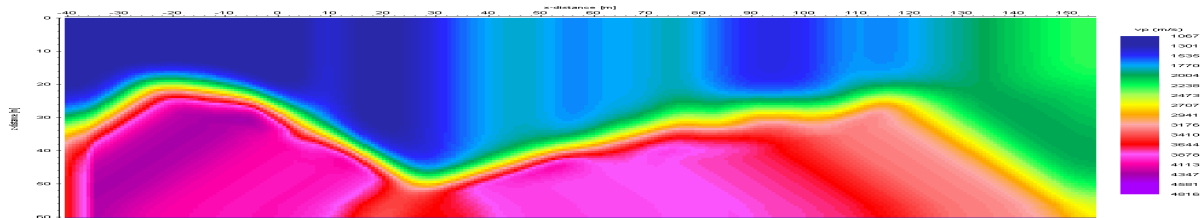


Figure 8: (a) Initial 2-D model with the corresponding ray-trace for profile L6 and (b) the final 2-D model after ten iterations.

(a)



(b)



(c)

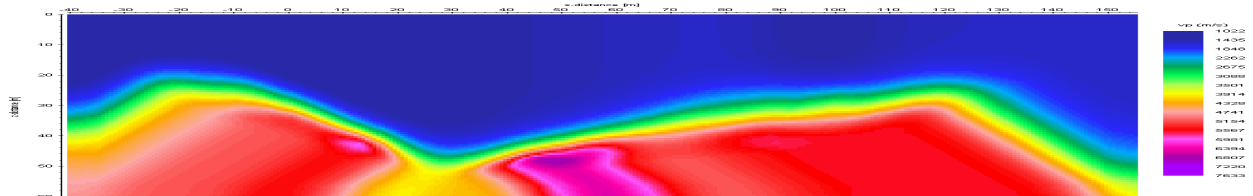
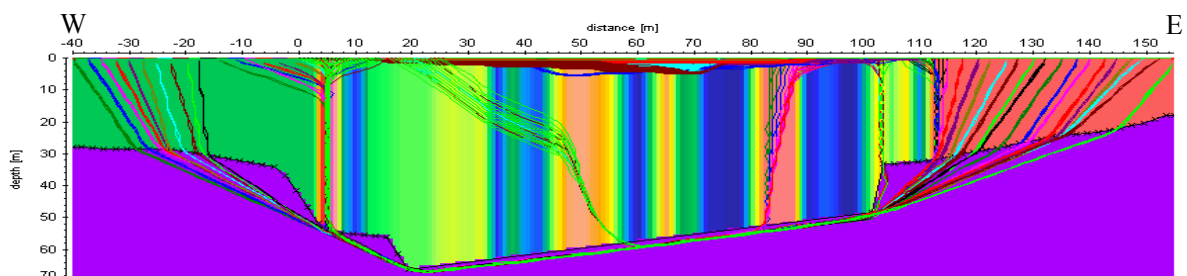


Figure 9: (a) Ray trace after editing model parameters (b) 2-D model after five iterations, and (c) final 2-D model after ten iterations.

(a)



(b)

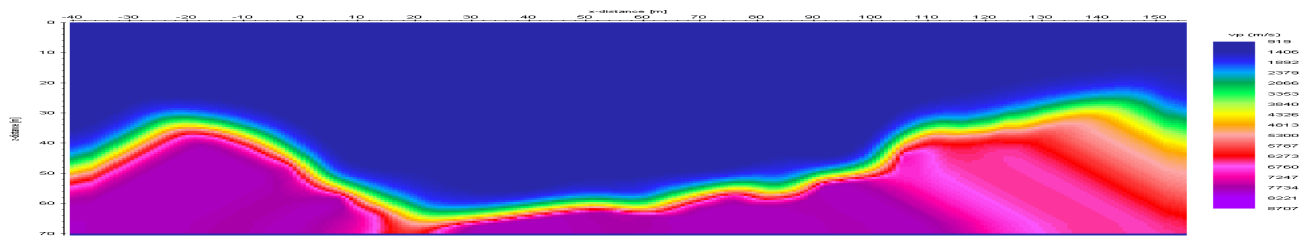
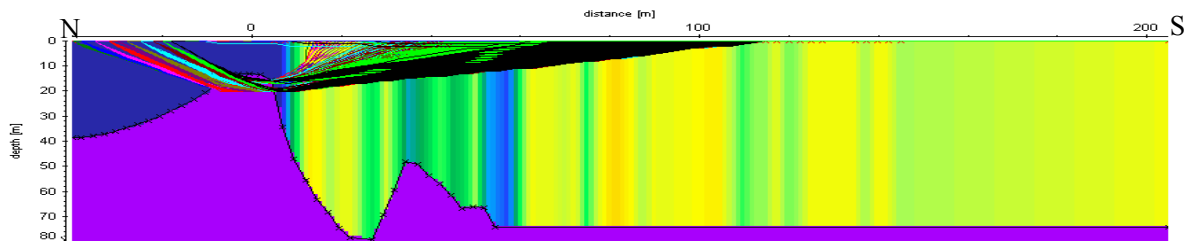


Figure 10: 2-D velocity model for profile L4 (a) initial 2-D model with the ray-trace before editing model parameters, and (b) after editing model parameters.

(a)



(b)

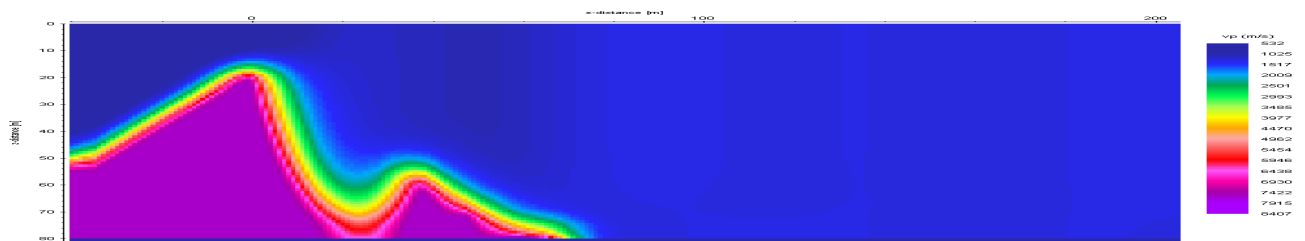
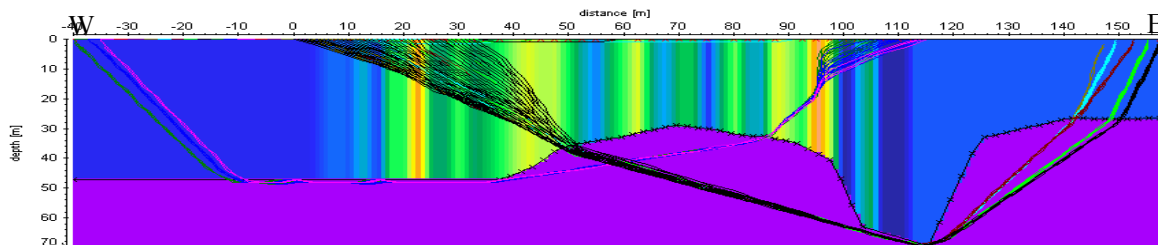


Figure 11: 2-D velocity model for profile L1 (a) initial 2-D model with the ray-trace, and (b) final 2-D velocity after ten iterations.

(a)



(b)

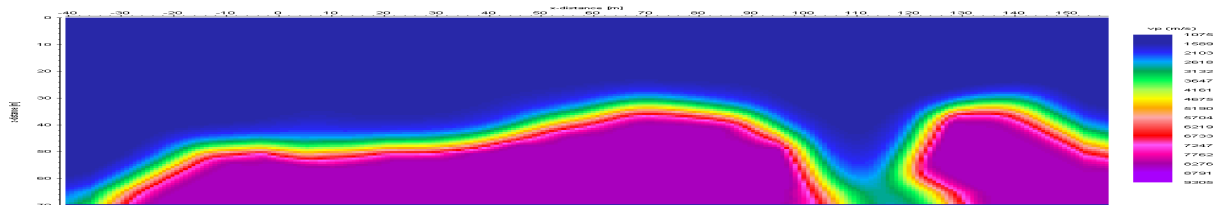
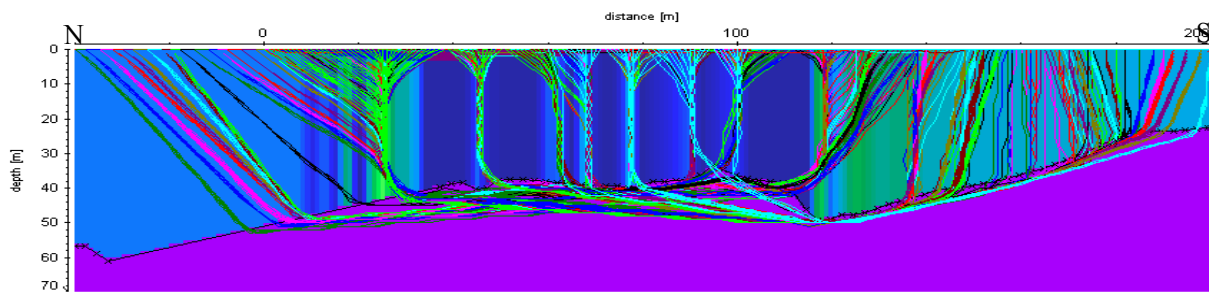


Figure 12: 2-D velocity model for profile L5 (a) initial 2-D model with the ray-trace, (b) final 2-D velocity model after ten iterations, with fracture zone towards the eastern part.

(a)



(b)

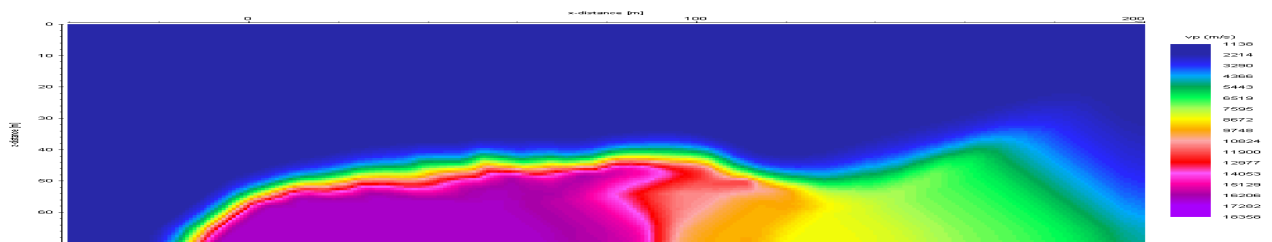
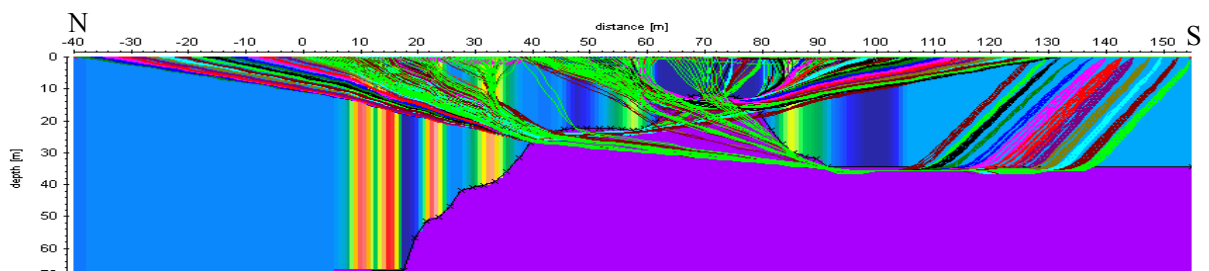


Figure 13: 2-D velocity model for profile L2 (a) initial 2-D model with ray-trace, and (b) final 2-D model after ten iterations.

(a)



(b)

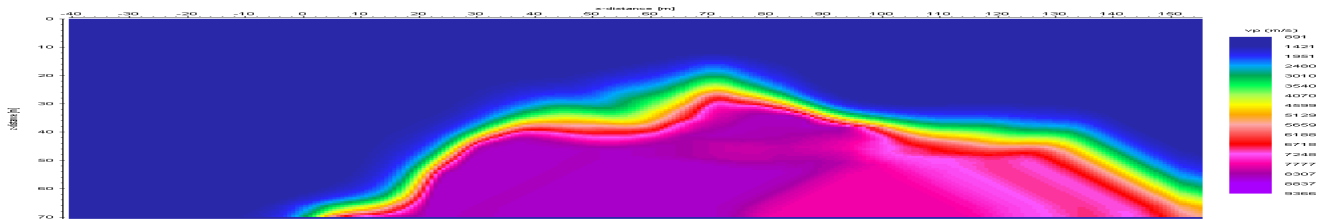


Figure 14: 2-D velocity model for profile L3 (a) initial 2-D model with ray-trace, and (b) final 2-D model after ten iterations.

Table I: Model parameters for the initial 2-D model.

(a) First layer			(b) Second layer		
Distance(m)	Depth(m)	P-wave velocity(m/s)	Distance(m)	Depth(m)	P-wave velocity(m/s)
-40.00	0.00	1193.85	-40.00	17.27	2512.39
2.50	0.00	1193.85	-38.50	17.27	2512.39
5.00	0.00	795.90	-36.50	17.57	2512.39
7.50	0.00	1198.00	-34.50	17.75	2512.39
10.00	0.00	1836.69	-32.50	17.82	2512.39
12.50	0.00	83572.34	-30.50	17.82	2512.39
15.00	0.00	1193.85	55.50	39.19	2512.39
17.5	0.00	1256.68	57.50	38.50	2512.39
20.00	0.00	1193.85	63.50	35.65	2512.39
22.50	0.00	1392.82			
25.00	0.00	1215.55			
27.50	0.00	1485.68			
30.00	0.00	1390.89			
32.50	0.00	1690.66			

Table II: The variation of overburden thickness in profile L1 to L5

Profiles	Overburden thickness
L1	Varies from about 18 m in the northern part to about 60 m towards the Southern part.
L2	Shows uniform thickness of about 40 m from the northern part to the southern part of the profile.
L3	Varies from 60 m in the northern part to 18 m at the centre and 50 m towards the southern part.
L4	Varies from 30 m in the western part to 55 m at the centre and 30 m towards the eastern part.
L5	Increases from 50 m in the western part to about 60 m towards the eastern part.